Reprinted from

FINITE ELEMENTS IN ANALYSIS AND DESIGN

Finite Elements in Analysis and Design 19 (1995) 181–194

A layerwise beam element for analysis of frames with laminated sections and flexible joints

Julio F. Davalos[a,*], Youngchan Kim[a], Ever J. Barbero[b]

[a] *Department of Civil Engineering, West Virginia University, Morgantown, WV 26506, USA*
[b] *Department of Mechanical and Aerospace Engineering, West Virginia University, USA*

ELSEVIER

ELSEVIER

Finite Elements in Analysis and Design 19 (1995) 181–194

FINITE ELEMENTS IN ANALYSIS AND DESIGN

A layerwise beam element for analysis of frames with laminated sections and flexible joints

Julio F. Davalos[a,*], Youngchan Kim[a], Ever J. Barbero[b]

[a] Department of Civil Engineering, West Virginia University, Morgantown, WV 26506, USA
[b] Department of Mechanical and Aerospace Engineering, West Virginia University, USA

Abstract

Fiber-reinforced plastic (FRP) composites are being used currently as reinforcement for beams of conventional materials, such as concrete and glued-laminated timber (glulam). The common assumption of plane cross-sections through the laminate for laminated beams with dissimilar ply stiffnesses can lead to inaccurate results, particularly for rectangular sandwich beams with soft cores. In this paper, we extend the formulation of a 3-node beam finite element with layerwise constant shear (BLCS) to the analysis of plane frames with rectangular laminated sections and flexible joints. Experimental results for sandwich beams and glulam-FRP beams are used to illustrate the accuracy of BLCS. An A-frame with two distinct laminated cross-sections and a rigid or flexible apex-joint is analyzed with BLCS and also plane-stress and layered-shell elements of ANSYS. The BLCS element predicts the response of the A-frame accurately and does not exhibit shear-locking.

Keywords: Composite material; Beam element; Frame analysis; Layerwise beam theory; Soft-core beam; Sandwich beam

1. Introduction

A recent application of advanced composite materials, primarily fiber-reinforced plastic (FRP) composites, in civil engineering structures is the reinforcement of conventional materials, such as concrete and glued-laminated timber (glulam), to increase their performance. The reinforcement of concrete and glulam beams has been explored either as a rehabilitation technique or as a means of reducing the depth of a member, which in turn can reduce the weight and the bracing requirements to prevent lateral buckling. Because of corrosion problems and as an alternative to the use of steel plates for strengthening purposes, glass fiber-reinforced plastic (GFRP) plates were bonded to the tension face of reinforced concrete beams [1]. Similarly, wood beams were reinforced with non-prestressed or prestressed epoxy-bonded carbon fiber-reinforced plastic (CFRP) sheets [2, 3].

* Corresponding author.

SSDI 0168-874X(95)00011-9

More recently, Davalos et al. [4] bonded pultruded GFRP laminates to glulam beams with a resorcinol–formaldehyde adhesive and obtained promising results.

In particular, the construction of large-scale glulam structures usually requires members with large depths [5, 6], and to significantly increase the stiffness and strength of glulam, the members can be reinforced with FRP at top and bottom surfaces. However, since the stiffness of the FRP face layers can be four to ten times greater than that of the wood core, glulam-FRP laminates are sandwich beams with relatively soft cores, and for these laminates, the common beam theory assumption of plane cross-sections through the laminate may not apply. Thus, when explicit solutions are used for sandwich beam analysis, the bending stiffness of the core and the shear deformation of the faces are usually neglected [7, 8]. The finite element models for sandwich plates are reviewed by Ha [9].

The behavior of laminated composite beams has been studied analytically and experimentally by various investigators, as summarized by Kapania and Raciti [10]. Based on the generalized laminate plate theory (GLPT) [11], we present in this paper an overview of the formulation of a 3-node beam finite element with layerwise constant shear (BLCS), which is equivalent to a first-order shear deformation beam theory (Timoshenko's beam) on each layer. While retaining the simplicity of a beam theory, the BLCS element gives results as accurate as much more complex three-dimensional elasticity analyses. The layerwise linear representation of in-plane displacements permits accurate computation of normal and shear stresses on each layer for laminated beams with dissimilar ply stiffnesses. For the accurate computation inter- and intra-laminar shear stresses, the constant shear stress on each layer is approximated by a quadratic function in a post-processing operation. The displacements are formulated with respect to an arbitrary reference axis, and therefore BLCS is basically a one-dimensional element suitable to model complex frame-type structures.

The accuracy of BLCS is evaluated by comparing the predicted displacements and stresses with test results for laminated sandwich beams and glulam-GFRP beams. For the static analysis of plane frames, we introduce rotational degrees of freedom in the formulation and present details of the derivation of the global element stiffness matrix. To model flexible joints, a rotational spring element is used, and several options to distribute the spring stiffness through the laminate are discussed. An A-frame with laminated members and a rigid or flexible apex-joint is analyzed, and the results are compared to predictions with plane-stress and layered-shell elements of the commercial program ANSYS [12].

2. Layerwise constant shear beam theory

The formulation of the beam element with layerwise constant shear (BLCS) is reviewed briefly to explain the derivation of the global stiffness matrix. The details of the theory can be found in Ref. [13]. The kinematic assumptions used in BLCS are transverse incompressibility and linear variation of in-plane displacements through the thickness. The displacements of a point (x–z plane) in the laminated beam are expressed as (Fig. 1)

$$u_1(x,z) = u(x) + \sum_{j=1}^{n} U^j(x)\phi^j(z), \qquad u_2(x,z) = w(x), \tag{1}$$

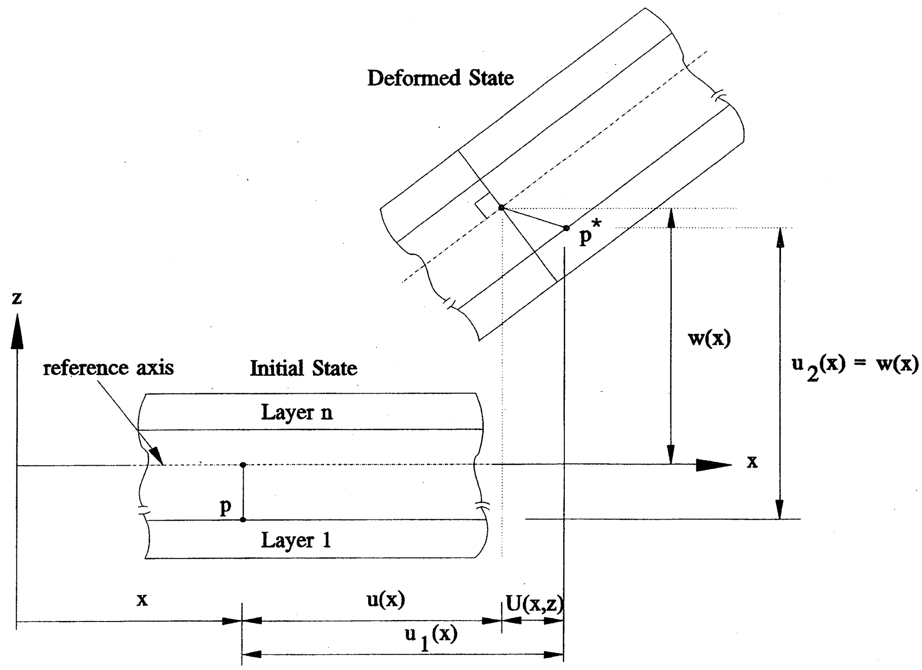

Fig. 1. Displacement components of a point p in the laminate.

where u and w are, respectively, the longitudinal and transverse displacements of a point on the reference axis of the laminate, and $U^j(x)$ represent layerwise in-plane displacements approximated by linear Lagrange interpolation functions $\phi^j(z)$. To represent the state of stress in each cross-ply lamina, the following approximations are used: $\sigma_y = \sigma_{xy} = \sigma_{yz} = 0$. Using these approximations and the transformed stress–strain relation of an orthotropic lamina under the assumption of plane stress in the x–y plane, the constitutive relation of a lamina is derived. Using the laminae constitutive relations and integrating stresses through the thickness, the constitutive equation of the laminate is established. In the finite element formulation of BLCS, the strain–displacement relation of an m-node element is defined as

$$\{\Delta^0\}^{\mathrm{T}} = \{u_1 \; w_1 \; \ldots \; u_m \; w_m\}, \quad \{\Delta^j\} = \{U^j\}, \quad \{\varepsilon^0\} = [B_L]\{\Delta^0\}, \quad \{\varepsilon^j\} = [\bar{B}_L]\{\Delta^j\},$$

where the superscripts 0 and j refer, respectively, to quantities at the reference axis and the laminae interfaces, and $[B_L]$ and $[\bar{B}_L]$ are compatibility matrices expressed in terms of interpolation functions. Applying the principle of virtual work, the N-layer element model is obtained as follows:

$$\frac{1}{b}\begin{Bmatrix} \{F\} \\ \{F_x^j\} \end{Bmatrix} = \begin{bmatrix} [A_1] & [B_i] \\ [B_i]^{\mathrm{T}} & [D_{ij}] \end{bmatrix} \begin{Bmatrix} \{\Delta^0\} \\ \{\Delta^j\} \end{Bmatrix} \quad \text{for } i, j = 1, 2, \ldots, N$$

or

$$\{f\} = [k]\{d\}, \tag{2}$$

where b is the beam width, $\{F\}$ includes transverse and axial force vectors applied at the reference axis, $\{F_x^j\}$ contains axial force vectors applied at the laminae interfaces, and the submatrices are defined as

$$[A_1] = \int_0^L [B_L]^{\mathrm{T}} [A] [B_L] \, \mathrm{d}x, \quad [B_i] = \int_0^L [B_L]^{\mathrm{T}} [B^i] [\bar{B}_L] \, \mathrm{d}x, \quad [D_{ij}] = \int_0^L [\bar{B}_L]^{\mathrm{T}} [D^{ij}] [\bar{B}_L] \, \mathrm{d}x,$$

The number of degrees of freedom per element is $(2 + N)m$. In a post-processing operation, the constant shear stress on each layer is converted into a parabolic shear stress distribution.

3. Formulation of the global stiffness matrix

The translational degrees of freedom (dof) in BLCS are u, w, and U^j (Fig. 1). For convenience, the relative in-plane local displacements U^j are transformed into rotational dof by simple geometric transformations. For example, for a 4-layer laminate this transformation can be expressed as follows (Fig. 2):

$$\begin{Bmatrix} U^1 \\ U^2 \\ U^3 \\ U^4 \end{Bmatrix} = \begin{bmatrix} -t_1 & -t_2 & 0 & 0 \\ 0 & -t_2 & 0 & 0 \\ 0 & 0 & t_3 & 0 \\ 0 & 0 & t_3 & t_4 \end{bmatrix} \begin{Bmatrix} \theta^1 \\ \theta^2 \\ \theta^3 \\ \theta^4 \end{Bmatrix},$$

where t_i ($i = 1,4$) is the lamina thickness. Similarly, for a 3-node beam element with N-layers, the dof can be transformed as

$$\begin{bmatrix} \{U^1\} \\ \{U^2\} \\ \cdot \\ \cdot \\ \{U^r\} \\ \{U^{r+1}\} \\ \cdot \\ \cdot \\ \{U^{N-1}\} \\ \{U^N\} \end{bmatrix} = \begin{bmatrix} -[T_1] & -[T_2] & \cdot\ \cdot & -[T_r] & [0] & \cdot & \cdot & \cdot & [0] \\ [0] & -[T_2] & \cdot\ \cdot & -[T_r] & [0] & \cdot & \cdot & \cdot & [0] \\ \cdot & \cdot & \cdot\ \cdot & \cdot & \cdot & \cdot & \cdot & \cdot & \cdot \\ \cdot & \cdot & \cdot\ \cdot & \cdot & \cdot & \cdot & \cdot & \cdot & \cdot \\ [0] & \cdot & \cdot\ \cdot & -[T_r] & [0] & \cdot & \cdot & \cdot & [0] \\ [0] & \cdot & \cdot\ \cdot & [0] & [T_{r+1}] & [0] & \cdot & \cdot & [0] \\ \cdot & \cdot & \cdot\ \cdot & \cdot & \cdot & \cdot & \cdot & \cdot & \cdot \\ \cdot & \cdot & \cdot\ \cdot & \cdot & \cdot & \cdot & \cdot & \cdot & \cdot \\ [0] & \cdot & \cdot\ \cdot & [0] & [T_{r+1}] & \cdot & \cdot & [T_{N-1}] & [0] \\ [0] & \cdot & \cdot\ \cdot & [0] & [T_{r+1}] & \cdot & \cdot & [T_{N-1}] & [T_N] \end{bmatrix} \begin{bmatrix} \{\theta^1\} \\ \{\theta^2\} \\ \cdot \\ \cdot \\ \{\theta^r\} \\ \{\theta^{r+1}\} \\ \cdot \\ \cdot \\ \{\theta^{N-1}\} \\ \{\theta^N\} \end{bmatrix},$$

or

$$\{\{U^j\}\} = [T]\{\{\theta^j\}\}, \tag{3}$$

where $r = N/2$; $[0] = 3 \times 3$ null matrix, and the vectors and submatrices are

$$\{U^j\} = \begin{Bmatrix} U_1^i \\ U_2^i \\ U_3^i \end{Bmatrix}, \quad \{\theta^i\} = \begin{Bmatrix} \theta_1^i \\ \theta_2^i \\ \theta_3^i \end{Bmatrix}, \quad [T_i] = \begin{bmatrix} t_i & 0 & 0 \\ 0 & t_i & 0 \\ 0 & 0 & t_i \end{bmatrix}.$$

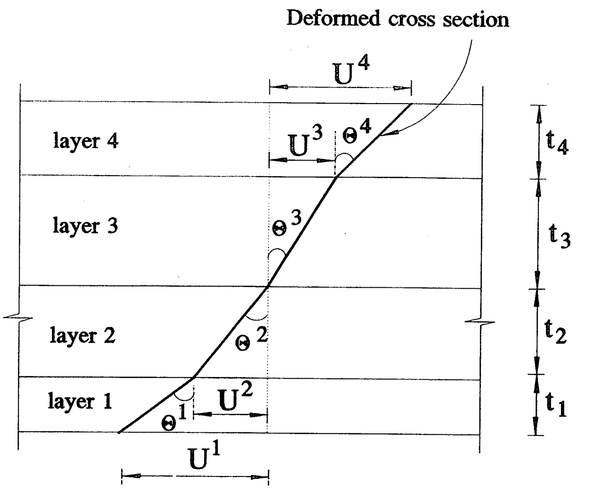

Fig. 2. In-plane translational and rotational dof in a 4-layer laminate.

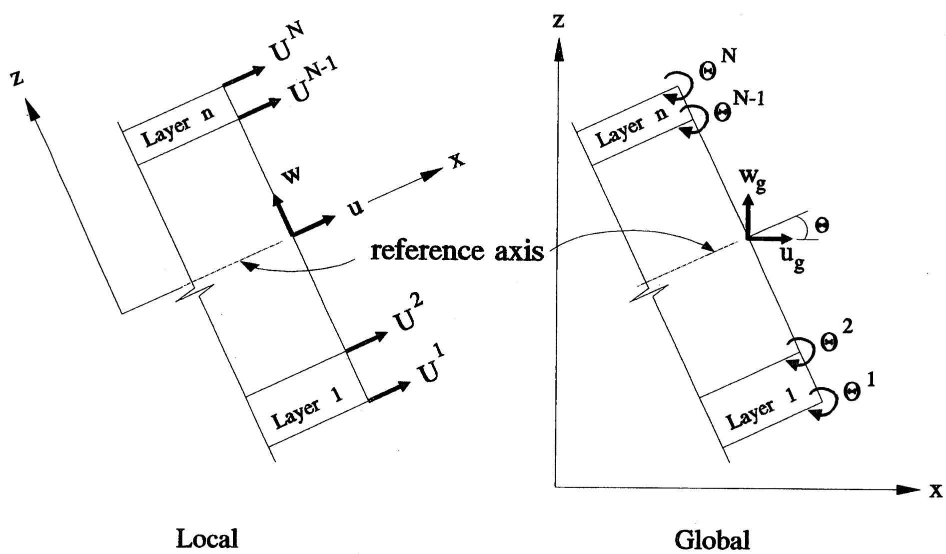

Fig. 3. Local and global degrees of freedom in BLCS.

For an m-node element, the local displacements at the reference axis, $\{\Delta^0\}$, are transformed into global quantities using a matrix $[R]$ (Fig. 3):

$$\{\Delta^0\} = [R]\{\Delta\}, \tag{4}$$

where

$$\{\Delta\}^{\mathrm{T}} = \{u_{\mathrm{g}}^1 \; w_{\mathrm{g}}^1 \; \ldots \; u_{\mathrm{g}}^m \; w_{\mathrm{g}}^{\mathrm{m}}\}.$$

For a 3-node beam element, $[R]$ becomes

$$\begin{bmatrix} \cos\theta & \sin\theta & 0 & 0 & 0 & 0 \\ -\sin\theta & \cos\theta & 0 & 0 & 0 & 0 \\ 0 & 0 & \cos\theta & \sin\theta & 0 & 0 \\ 0 & 0 & -\sin\theta & \cos\theta & 0 & 0 \\ 0 & 0 & 0 & 0 & \cos\theta & \sin\theta \\ 0 & 0 & 0 & 0 & -\sin\theta & \cos\theta \end{bmatrix},$$

where θ is the angle between local and global axes. Then, the local force and local displacement vectors can be transformed into global terms as follows:

$$\{Q\} = [\Lambda]^{\mathrm{T}}\{f\}, \quad \{d\} = [\Lambda]\{D\}, \tag{5}$$

where $[\Lambda]$ is defined as

$$\begin{bmatrix} [R] & 0 \\ 0 & [T] \end{bmatrix}$$

and the global force and displacement vectors are

$$\{Q\} = \begin{Bmatrix} \{q\} \\ \{q_x^1\} \\ \cdot \\ \{q_x^N\} \end{Bmatrix}, \quad \{D\} = \begin{Bmatrix} \{\Delta\} \\ \{\theta^1\} \\ \cdot \\ \{\theta^N\} \end{Bmatrix}.$$

Finally, consistent with matrix formulations, the global element model is expressed as

$$\{Q\} = [\Lambda]^{\mathrm{T}}[k][\Lambda]\{D\} = [K]\{D\}, \tag{6}$$

where the local element stiffness matrix $[k]$ is given in Eq. (2), and the global element stiffness matrix $[K]$ is written as

$$\begin{bmatrix} [R]^{\mathrm{T}}[A_1][R] & [R]^{\mathrm{T}}[B_i][T] \\ [T]^{\mathrm{T}}[B_i]^{\mathrm{T}}[R] & [T][D_{ij}][T] \end{bmatrix}.$$

In addition to the global element stiffness matrix, a rotational spring element is used to analyze frames with flexible joints, as discussed next.

4. Connection modeling with spring elements

A rigid joint commonly assumed in structural analysis is seldom possible in sandwich beams, and a flexible joint can model the response more accurately. A rotational spring can simulate a flexible joint that transmits a moment proportional to the relative rotation of the spring. Following Holzer [14], the moment–rotation relation for a 2-dof spring element can be written as

$$f_1 = -f_2 = \gamma(\theta_1 - \theta_2), \tag{7}$$

where γ is spring stiffness (moment per unit radian), which represents the slope of the moment–rotation curve and can be found experimentally, as discussed in Ref. [15] for full-size tests of beam-to-column moment connections of glass–vinylester pultruded sections. Expressed in matrix form, Eq. (7) becomes

$$\begin{Bmatrix} f_1 \\ f_2 \end{Bmatrix} = \gamma \begin{bmatrix} 1 & -1 \\ -1 & 1 \end{bmatrix} \begin{Bmatrix} \theta_1 \\ \theta_2 \end{Bmatrix}.$$

In the BLCS formulation of element-to-element connection with spring elements, the nodes at the reference axis are connected, and the stiffness of the spring element is distributed through the laminae above and below the reference axis. Since rotational dof are provided at the laminae interfaces through the laminate thickness (Fig. 3), except at the reference axis, several approaches can be used to distribute the spring stiffness through the laminate thickness. Considering that the relative rotation of a beam section is proportional to its bending stiffness, the stiffness of the spring connector can be distributed layerwise in proportion to the bending stiffness of each layer. Then, the spring stiffness corresponding to the kth layer of an N-layer laminate can be expressed as

$$\gamma_k = \frac{E_x^k (t_k^3/12 + \bar{z}_k^2 t_k)}{\sum_{j=1}^{N} E_x^j (t_j^3/12 + \bar{z}_j^2 t_j)} \gamma, \tag{8}$$

where γ is the joint stiffness and $\bar{z}_k$ is the distance from the beam neutral axis to the centroid of the kth layer. Another possibility is to distribute the joint stiffness either uniformly or selectively through the laminate. This approach may be useful for sandwich beams with soft cores, for which the stiffness of the spring element can be distributed only to the top and bottom face laminae. We investigated several of these schemes and obtained similar results for various laminates. In the present study, the first method is used (Eq. (8)) for the analysis of an A-frame with flexible joints.

5. Numerical examples

The accuracy of the BLCS element is illustrated by analyzing the response of laminated beams and an A-frame with laminated sections and a rigid or flexible apex-joint. To evaluate the capabilities of BLCS to predict member response, we use experimental results for glued-laminated timber (glulam) beams reinforced with GFRP and experimental/analytical results for sandwich beams.

5.1. Member response

We present two examples to demonstrate the capability of the model to predict beam behavior.

1. Glulam-GFRP beams

Davalos et al. [4] conducted two-point bending tests of simply supported glulam beams reinforced with pultruded GFRP strips (Fig. 4). The material properties of the wood laminate given in Table 1 are the averages of six wood layers. The longitudinal and shear moduli of the GFRP are 19.7 and 3.80 GPa, respectively, and the thickness is 9.4 mm. The ratios shown in Table 2 are obtained by dividing the maximum displacements and tensile stresses of BLCS with those measured experimentally. The results show that the BLCS predictions agree closely with the experimental values.

2. Sandwich beams

The bending response of laminated sandwich beams is evaluated with ANSYS and BLCS. The beams were tested under two-point loading by Kemmochi and Uemura [16], who used photoelasticity to measure the stress distribution. The beam configuration and modeling of one half of the beam are given in Fig. 5. The material properties and load (p) are reported in Table 3 for two

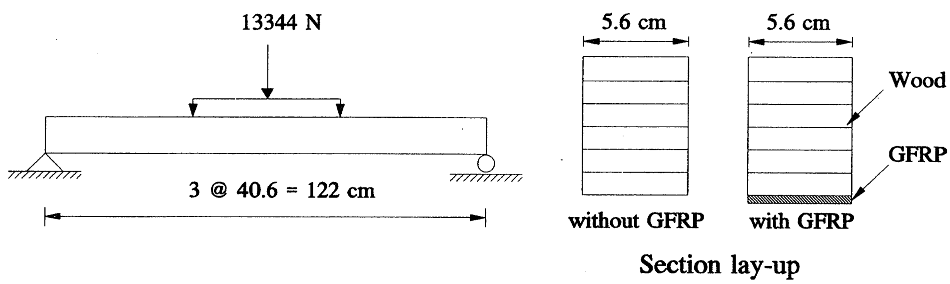

Fig. 4. Configuration of glulam-GFRP beams.

Table 1
Material properties of wood layers

Beam no.	E_{avg} (GPa)	G_{avg} (GPa)	t_{avg} (mm)
1	15.12	0.7	19.39
2	14.52	0.70	19.39
3	14.47	0.68	19.4
4	13.71	0.73	19.09

Table 2
Maximum displacement and stress ratios (BLCS/experimental)

Beam no.	Without GFRP		With GFRP	
	Displacement	Stress[a]	Displacement	Stress[b]
1	0.933	0.929	0.943	0.900
2	1.022	0.996	1.025	1.062
3	0.947	0.960	1.001	1.085
4	0.906	0.954	0.905	1.087

[a] Stresses are measured at the middle of the lower wood layer.
[b] Stresses are measured at the bottom of the GFRP layer.

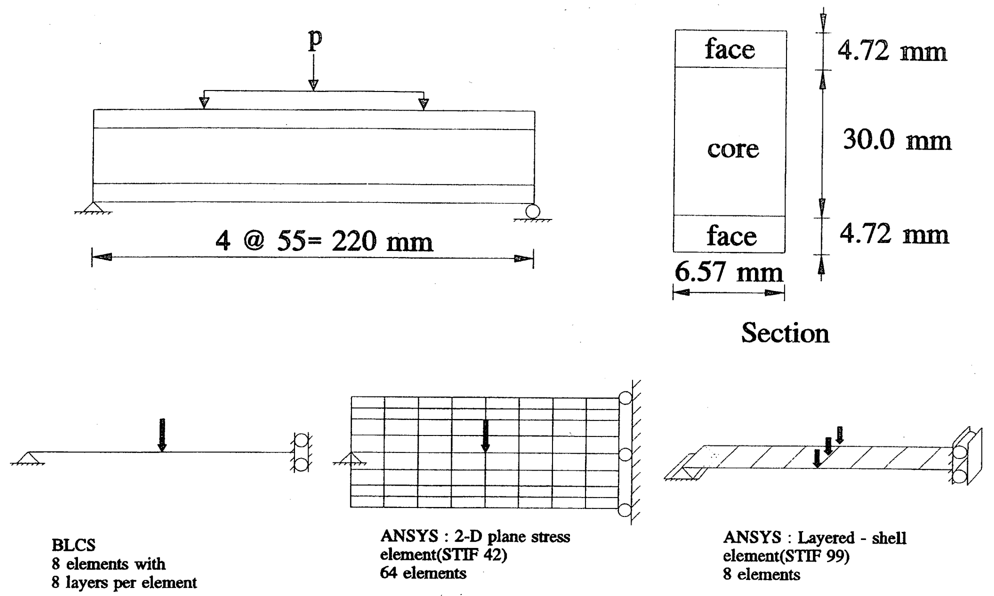

Fig. 5. Sandwich beam configuration and modeling.

Table 3
Material properties and loads

	Case A		Case B	
	Face	Core	Face	Core
E (MPa)	2440	521	2440	4.34
G (MPa)	875	181	875	0.53
p (N)	98		9.8	

material/load cases. Using the commercial program ANSYS, the beams are analyzed by two elements: (1) plane-stress, 4-node isoparametric element (STIF 42) and (2) Mindlin layered-shell, 8-node element (STIF 99). Because of its favorable bending characteristics, an 8-node plane-stress element (STIF 82) was initially used in the analysis, but similar results to those given by the 4-node element were obtained and, thereafter, the 4-node element was chosen in this study. The midspan maximum displacement and normal stress distribution are given in Table 4 and Fig. 6, respectively. The experimental displacements of the beams were not reported in Ref. [16]. For Case A, both BLCS and ANSYS predict values quite close to those of Kemmochi and Uemura. For the soft-core Case B, it is noticeable that the sign-change of normal stress within the face material cannot be accurately predicted with the layered-shell element. In addition, and more significantly, the Mindlin layered-shell element, which assumes first-order shear deformation through the cross-section, experiences "shear-locking" when the core material is soft. (The longitudinal and shear stiffness of the core for Case B are, respectively, 120 and 342 times lower than for Case A.) As indicated in Table 4, the Mindlin layered-shell element predicts a very stiff response.

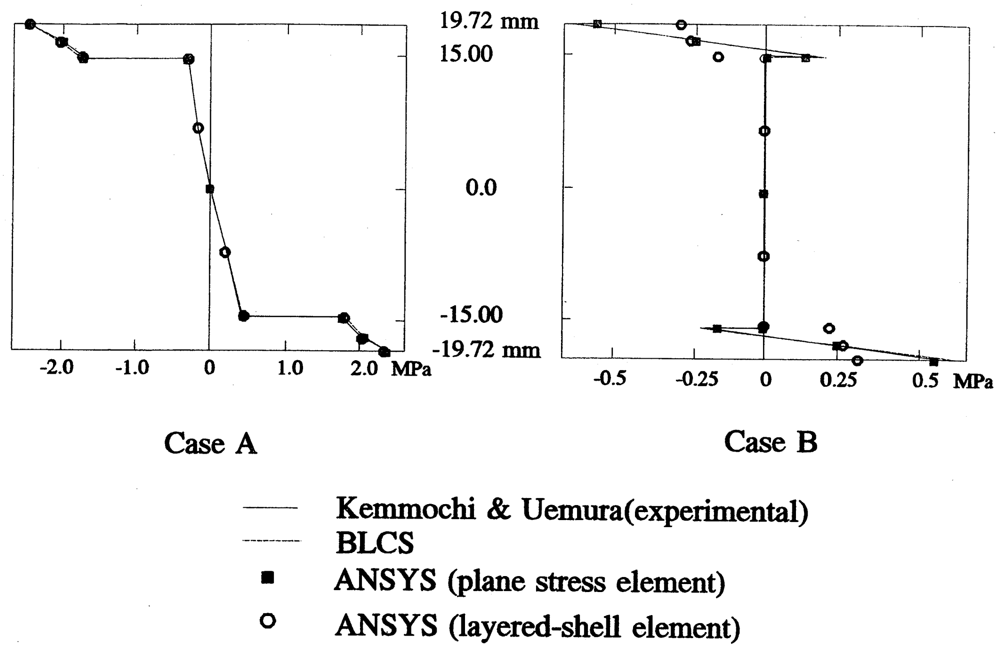

Fig. 6. Normal stress distribution at midspan.

Table 4
Comparison of maximum displacement (mm)

	BLCS	ANSYS	
		Plane stress	Layered-shell
Case A	0.35	0.35	0.31
Case B	0.76	0.74	0.04

5.2. *Frame response*

To evaluate the performance of the BLCS element in frame analysis, an A-frame with laminated cross-section and loaded at the apex with concentrated loads is examined (see Fig. 7). Two material lay-up configurations are used (Fig. 7 and Table 5): in Case 1 the material properties vary progressively through the depth, and in Case 2 the face material is much stiffer than the core material, and therefore Case 2 represents a soft-core sandwich member. The frame is modeled with BLCS using 16 elements with six layers per element; when modeling with ANSYS, we used 96 plane-stress elements and 16 layered-shell elements. The frame is modeled for a rigid connection and also a flexible connection at the apex. To simulate a flexible connection with BLCS the spring element described earlier (Eqs. (7) and (8)) is used; similarly, a spring element (STIF 27) is used in conjunction with the layered-shell element of ANSYS. Since the plane-stress element in ANSYS does not have a rotational dof, a spring element cannot be used in this case, and therefore the

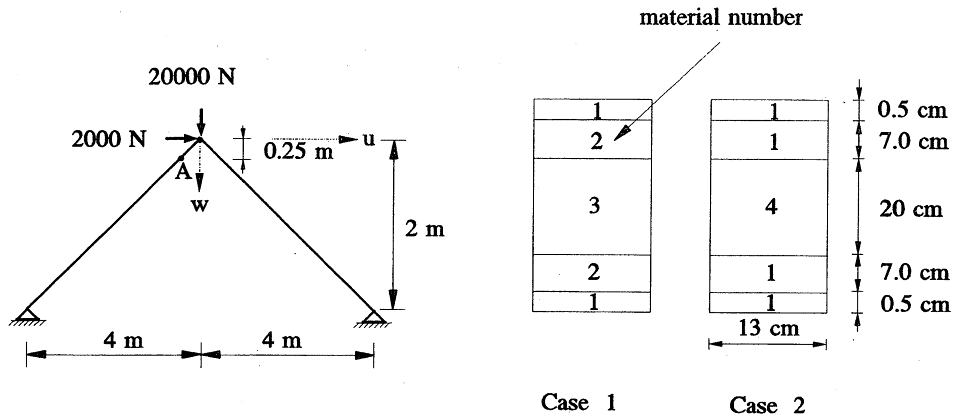

Fig. 7. Frame configuration and cross-sections.

Table 5
Material properties

Material no.	E (MPa)	G (MPa)
1	5000	800
2	1500	500
3	1100	400
4	110	80

Table 6
Displacements comparison (mm)

	Case 1					Case 2				
	Rigid joint			Flexible joint		Rigid joint			Flexible joint	
	BLCS	PS	LS	BLCS	LS	BLCS	PS	LS	BLCS	LS
u	0.109	0.104	0.090	0.109	0.090	0.303	0.248	0.056	0.303	0.056
w	3.938	3.970	3.559	4.357	3.584	6.958	7.19	2.205	12.14	2.223

PS = plane stress; LS = layered shell.

ANSYS plane-stress element is used only for the rigid-jointed Cases 1 and 2. The spring stiffness used for the analysis is 10^5 N m/rad. The displacements of the apex of the frame are given in Table 6, and the normal stress distributions at point A near the apex (Fig. 7) are shown in Fig. 8 for Case 1 and in Fig. 9 for Case 2.

For Case 1 with rigid joint, the plane-stress (PS) element and BLCS predict basically the same values for deflections u and w (see Fig. 7 and Table 6) and normal stress (Fig. 8), whereas the

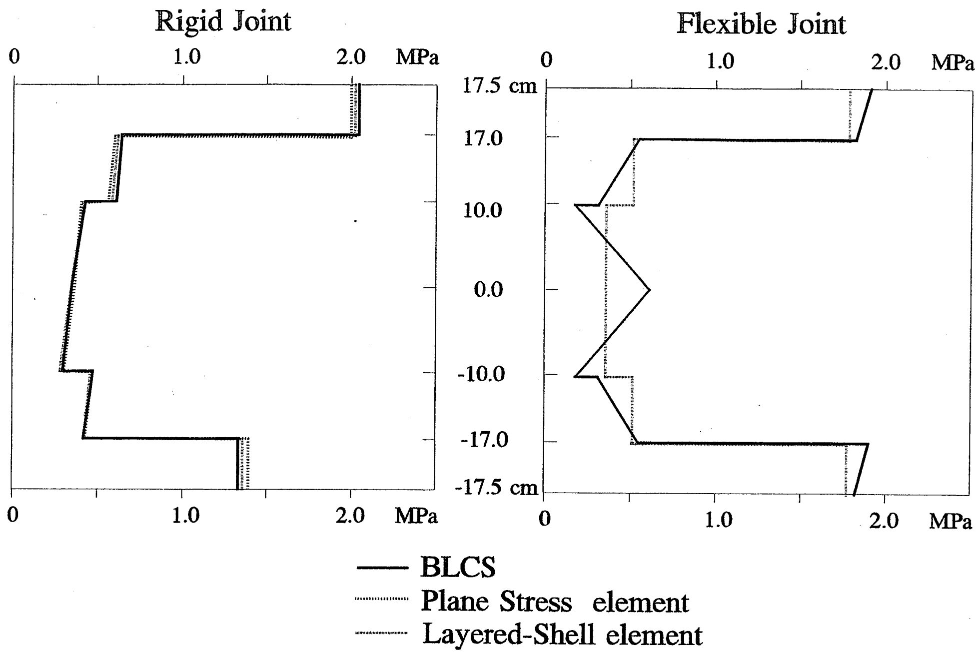

Fig. 8. Normal stress distribution at A for Case 1.

layered-shell element is slightly stiffer than the BLCS and PS elements, but the normal stress distribution at A coincides with BLCS and PS (Fig. 8). For Case 1 with flexible joint, the maximum vertical deflection given by the layered-shell element is 17% below the value given by BLCS (Table 6), and the distribution of normal stress (Fig. 8) with the layered-shell element is approximately constant on each layer consistent with the assumption of plane sections through the cross-section; in contrast, the layerwise formulation with BLCS can model the linear deformation on each layer more accurately.

For Case 2 with rigid joint, the deflection predictions with BLCS and PS are close to each other, but the layered-shell element locks and cannot predict the response of the frame (Table 6). Also, similar stress distribution are predicted with BLCS and PS (Fig. 9), but the stresses predicted with the layered-shell element are significantly different for the outer layers. For Case 2 with flexible joint, the layered-shell element exhibits an extremely stiff behavior and cannot predict the maximum deflection of the frame (Table 6), although the stress predictions follow the general trend of the BLCS stress distribution (Fig. 9).

The results obtained for Case B of the sandwich beam (see member-response study, Table 3) and Case 2 of the A-frame indicate that for soft-core laminates the assumption of plane sections through the cross-section can result in shear-locking and inaccurate stress predictions. It is shown that the BLCS element can accurately predict displacements and stresses for frames with soft-core laminated members, as verified with the plane-stress element of ANSYS.

Although the number of dof with BLCS is approximately the same as that of the plane-stress element, the BLCS mesh-definition is relatively simple and similar to that of a one-dimensional beam element. When flexible joints are included in the analysis of soft-core laminates, the shear-locking phenomenon with the Mindlin layered-shell element is exacerbated. Once again, the

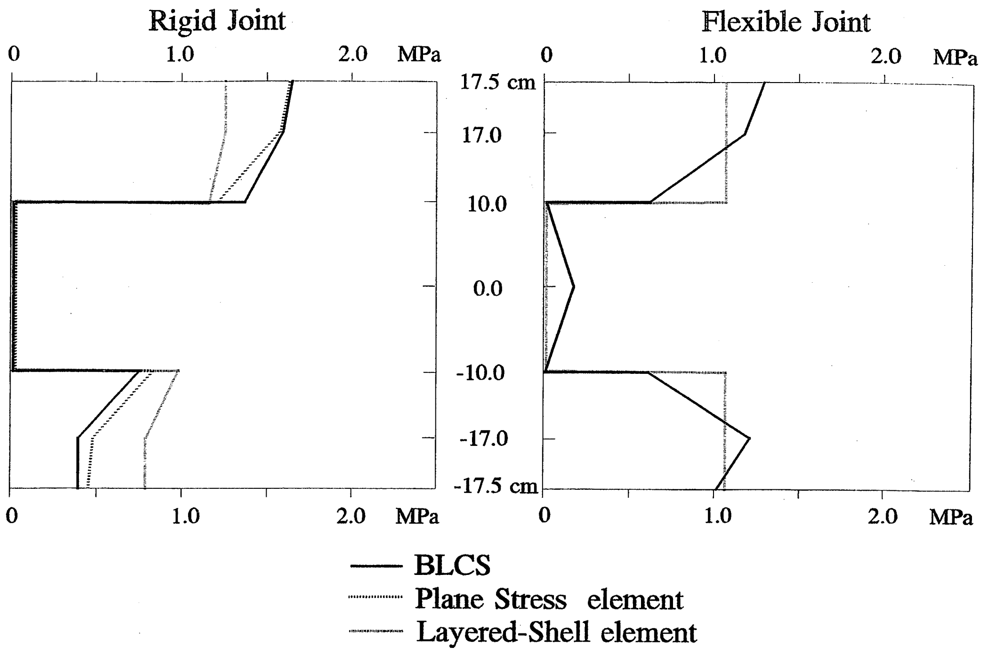

Fig. 9. Normal stress distribution at A for Case 2.

BLCS element can model the response with flexible joints and offers the flexibility of distributing the spring connector-stiffness in various ways through the laminate.

6. Summary and conclusion

The formulation of a 3-node beam finite element with layerwise constant shear (BLCS) is extended to the linear elastic analysis of plane frames with laminated rectangular sections and rigid or flexible joints. We discuss the derivation of the global element stiffness matrix, and the formulation of a rotational spring element used to model flexible joints. The BLCS element is particularly suited for the analysis of laminated sections with dissimilar ply stiffnesses, such as sandwich beams with soft cores.

Experimental results for reinforced laminated wood beams (glulam-GFRP) and sandwich beams are used to show the accuracy of the BLCS element to predict displacements and stresses. The laminated test-beams are also analyzed with plane-stress and Mindlin layered-shell elements of ANSYS. It is shown that for soft-core sandwich beams both BLCS and plane-stress elements predict values in agreement with the experimental results, but the layered-shell element, which assumes first-order shear deformation through the laminate cross-section, "locks" and cannot predict the response.

To illustrate the applicability of BLCS to frame analysis, an A-frame with two lay-up configurations and either rigid or flexible apex-joint is analyzed. For rigid apex-joint and laminates with either gradually varying stiffness or soft-core configuration, BLCS and the plane-stress element of ANSYS predict close results. In contrast, for the case of soft-core laminate, the layered-shell element of ANSYS predicts inaccurate results for rigid and flexible apex-joints. Because of the layerwise linear formulation, BLCS can efficiently model plane frames with soft-core laminates and flexible joints. The BLCS formulation offers the flexibility of distributing the connector spring-stiffness either selectively or uniformly through the cross-section laminae. In this paper, an expression is provided to distribute the spring stiffness in proportion to the bending stiffness of each layer.

References

[1] H. Saadtmanesh and M.R. Ehsani, "RC beams strengthened with GFRP: experimental study", *J. Struct. Eng.* **117**, pp. 3417–3433, 1991.

[2] T.C. Triantafillou and N. Deskovic, "Prestressed FRP sheets as external reinforcement of wood members", *J. Struct. Eng.* **118**, pp. 1270–1284, 1992.

[3] N. Plevris and T. Triantafillou, "FRP-reinforced wood as structural material", *J. Mater. Civ. Eng.* **4**, pp. 300–317, 1992.

[4] J.F. Davalos, H.A. Salim and U. Munipalle, "Glulam-GFRP composite beams for stress-laminated T-system bridges", *Proc. 1st Int. Conf. of Advanced Composite Materials in Bridges and Structures*, CSCE-CGC, Sherbrooke (Quebec), Canada, pp. 455–464, 1992.

[5] S.M. Holzer, J.F. Davalos and C.Y. Huang, "A review of finite element stability investigation of spatial wood structures", *Bull. Int. Assoc. Shell Spatial Struct.* **31**, pp. 161–171, 1991.

[6] J.F. Davalos, Y. Kim and S.S. Somnath, "Analysis of glulam-FRP beams by a layer-wise formulation", *Proc. IASS-ASCE Int. Symp. '94*, Atlanta, Georgia, pp. 67–75, 1994.

[7] R.A. DiTaranto, "Static analysis of a laminated beam", *J. Eng. Ind.* **95**, pp. 755–761, 1973.

[8] K.H. Ha and L.S. Salvador, "Stiffness matrices for exact analysis of sandwich beam systems", *Proc. 2nd Int. Conf. on Sandwich Construction*, **1**, pp. 67–89, 1992.

[9] K.H. Ha, "Finite element analysis of sandwich plates: an overview", *Comput. Struct.* **37**, pp. 397–403, 1990.

[10] R.K. Kapania and S. Raciti, "Recent advances in analysis of laminated beams and plates. Part 1: shear effect and buckling", *AIAA J.* **27**, pp. 923–934, 1989.

[11] J.N. Reddy, "A generalization of two-dimensional theories of laminated composite plates", *Commun. Appl. Numer. Methods* **3**, pp. 173–180, 1987.

[12] *ANSYS User's Manual*, Swanson Analysis System Inc., Houston, PA, 1989.

[13] Y. Kim, J.F. Davalos and E.J. Barbero, "Composite beam element with layerwise plane sections", *J. Eng. Mech. ASCE* **120** (5), pp. 1160–1166, 1994.

[14] S.M. Holzer, *Computer Analysis of Structures*, Elsevier, New York, 1985.

[15] L.C. Bank and A.S. Mosallam, "Performance of pultruded FRP beam-to-column connections", *Proc. ASCE Struct. Congr.'91*, pp. 389–392, 1991.

[16] K. Kemmochi and M. Uemura, "Measurement of stress distribution in sandwich beams under four-point bending", *Exp. Mech.* **20**, pp. 80–86, 1980.